



Citation for published version:

Wu, X, Price, GJ & Guy, RH 2009, 'Disposition of nanoparticles and an associated lipophilic permeant following topical application to the skin', *Molecular Pharmaceutics*, vol. 6, no. 5, pp. 1441-1448.
<https://doi.org/10.1021/mp9001188>

DOI:

[10.1021/mp9001188](https://doi.org/10.1021/mp9001188)

Publication date:

2009

Document Version

Peer reviewed version

[Link to publication](#)

This document is the Accepted Manuscript version of a Published Work that appeared in final form in *Molecular Pharmaceutics*, copyright © American Chemical Society after peer review and technical editing by the publisher. To access the final edited and published work see <http://dx.doi.org/10.1021/mp9001188>

University of Bath

Alternative formats

If you require this document in an alternative format, please contact:
openaccess@bath.ac.uk

General rights

Copyright and moral rights for the publications made accessible in the public portal are retained by the authors and/or other copyright owners and it is a condition of accessing publications that users recognise and abide by the legal requirements associated with these rights.

Take down policy

If you believe that this document breaches copyright please contact us providing details, and we will remove access to the work immediately and investigate your claim.

Disposition of nanoparticles and an associated lipophilic permeant following topical application to the skin

Journal:	<i>Molecular Pharmaceutics</i>
Manuscript ID:	mp-2009-001188.R1
Manuscript Type:	Article
Date Submitted by the Author:	
Complete List of Authors:	Wu, Xiao; University of Bath, Pharmacy & Pharmacology Price, Gareth; University of Bath, Department of Chemistry Guy, Richard; University of Bath, Pharmacy & Pharmacology



1
2
3
4
5
6
7
8
9
10
11
12
13
14
15
16
17
18
19
20
21
22
23
24
25
26
27
28
29
30
31
32
33
34
35
36
37
38
39
40
41
42
43
44
45
46
47
48
49
50
51

Disposition of Nanoparticles and an Associated Lipophilic Permeant following Topical Application to the Skin

Xiao Wu¹, Gareth J. Price² and Richard H. Guy^{1,*}

¹*Department of Pharmacy and Pharmacology, University of Bath, Claverton Down, Bath, BA2 7AY, U.K.*

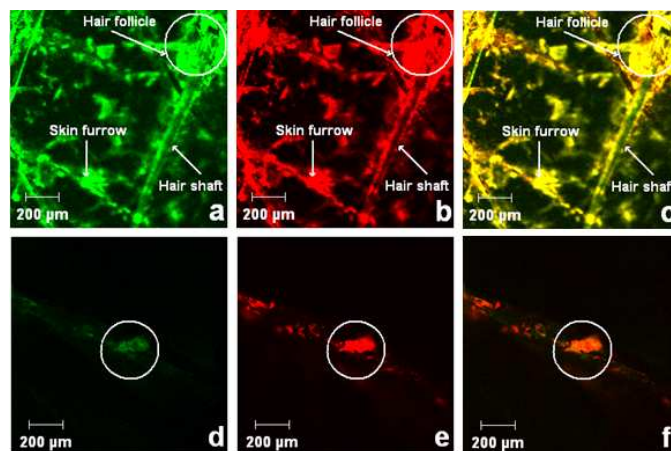
²*Department of Chemistry, University of Bath, Claverton Down, Bath, BA2 7AY, U.K.*

Running title: Disposition of Polymeric Nanoparticles on Skin

52
53
54
55
56
57
58
59
60

* To whom correspondence should be addressed. R.H.G.: Department of Pharmacy and Pharmacology,
University of Bath, Claverton Down, Bath, BA2 7AY, U.K.; phone, +44.1225.384901; fax, +44.1225.386114;
e-mail, r.h.guy@bath.ac.uk.

1
2
3
4 For Table of Contents Use Only
5
6
7
8



Manuscript title: Disposition of Nanoparticles and an Associated Lipophilic Permeant following Topical

Application to the Skin

Authors: Xiao Wu, Gareth J. Price and Richard H. Guy

1
2
3
4 **Abstract:** The objective was to determine the disposition of polymer nanoparticles and an
5
6 associated, lipophilic, model “active” component on and within the skin following topical
7
8 application. Polystyrene and poly(methyl methacrylate) nanoparticles containing covalently
9
10 bound fluorescein methacrylate and dispersed Nile Red were prepared by emulsion
11
12 polymerization. The two fluorophores differentiate the fate of the polymeric vehicle on and
13
14 within the skin from that of the active. Nanoparticles were characterized by dynamic light
15
16 scattering, transmission electron microscopy and NMR spectroscopy. In-vitro skin
17
18 permeation experiments were performed using dermatomed porcine skin. Post-treatment
19
20 with nanoparticle formulations, the skin surface was either cleaned carefully with buffer, or
21
22 simply dried with tissue, and then immediately visualized by confocal microscopy. Average
23
24 nanoparticle diameters were below 100 nm. Confocal images showed that nanoparticles
25
26 were located in skin “furrows” and around hair follicles. Surface cleaning removed the
27
28 former but not all of the latter. At the skin surface, Nile Red remained partly associated
29
30 with nanoparticles, but was also released to some extent and penetrated into deeper layers
31
32 of the stratum corneum (SC). In summary, polymeric nanoparticles did not penetrate
33
34 beyond the superficial SC, showed some affinity for hair follicles, and released an
35
36 associated “active” into the skin.
37
38
39
40
41
42
43
44
45
46
47
48
49
50
51

52 **Keywords:** Nanoparticles; skin; laser scanning confocal microscopy (LSCM); topical drug
53
54 delivery.
55
56
57
58
59
60

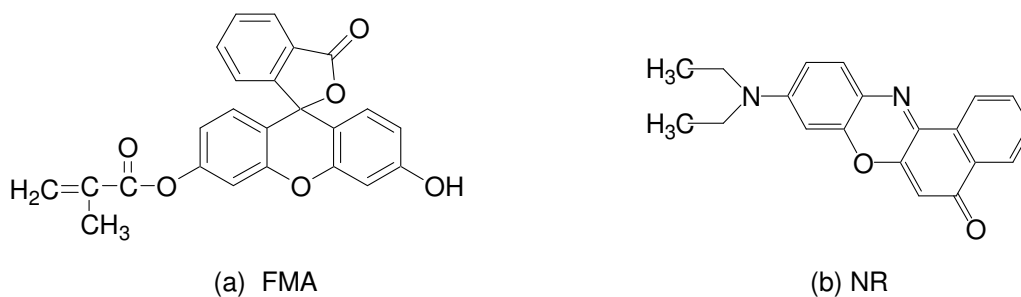
Introduction

Recently, polymeric nanoparticles (NP) have been proposed as carriers for drugs and other active agents administered by topical administration. Examples include anti-inflammatory drugs,^{1,2} anti-infective drugs, vitamins³ and sunscreens.⁴⁻⁶ It has been claimed that drug-loaded NP achieve sustained release and consequently improve the therapeutic effect of dermatological formulations.^{2,3} More importantly, NP can increase the stability of sensitive actives by protecting the molecules in a polymeric shell. Based on this, NP have been incorporated into several commercially available cosmetic products to encapsulate various actives (e.g., vitamin A, rose extract and wheat germ oil).

The development of topical formulations containing nano-sized materials has also been challenged by mechanistic and toxicity issues. Compared with larger particles, it has been suggested that nanostructures are more likely to penetrate the stratum corneum and gain access to the living cells within the epidermis and dermis. Should this be possible, then systemic exposure might occur (i.e., the nanoparticles being taken up into the blood and distributed to various tissues and organs), presenting thereby a potential toxicity risk for human health.⁷⁻¹⁰ Therefore, understanding the topical disposition of both vehicle and active is essential for the use of nano-engineered topical formulations. Whether (and when) the active is released from the vehicle, and the fate of the vehicle itself, are very important questions concerning the safety of nanotechnology. To address these issues, two series of polymeric NP have been prepared in which the polymer was covalently-labelled with fluorescein methacrylate (FMA, Chart 1a). A second fluorescent compound, Nile Red (NR, Chart 1b) was incorporated into the particles to simulate a hydrophobic active. Laser scanning confocal microscopy (LSCM) was used to track both fluorophores after topical application to porcine skin.

1
2
3
4 Porcine skin is a good substitute for human skin having epidermal thickness, lipid composition,
5
6 permeability, transepidermal water loss and low frequency impedance values which are very
7
8 similar.^{11, 12}
9
10

11
12
13
14
15 **Chart 1.** Chemical structures of fluorescein methacrylate (FMA) and Nile Red (NR).



32 Materials and Methods

33
34
35 **Tissue.** Full thickness porcine skin was obtained from a local slaughterhouse. The skin was
36
37 cleaned carefully under cold running water. The subcutaneous fat was removed with a scalpel. The
38
39 remaining tissue was dermatomed to a thickness of ~750 μm . Finally, the dermatomed skin was
40
41 stored frozen at -20°C for up to a maximum of one month before use.
42
43
44

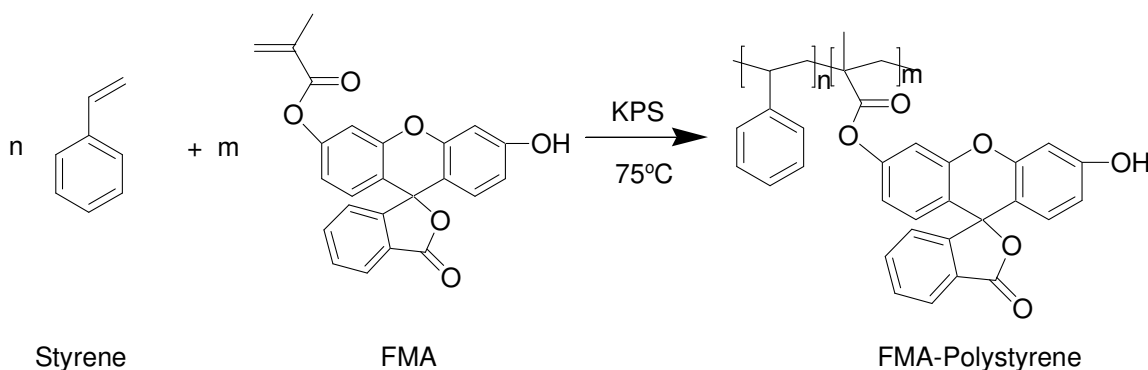
45
46 **Chemicals.** Fluorescein O-Methacrylate (97% pure), Nile Red (analytical grade) and
47
48 polystyrene (PS, MW: 44,000) were purchased from Sigma-Aldrich (St. Louis, MO, USA).
49
50 Styrene (99% GC), methyl methacrylate (MMA, 99% GC) and potassium persulfate (KPS) were
51
52 purchased from Sigma-Aldrich (Gillingham, Dorset, England). Other chemicals used were
53
54
55
56
57
58
59
60

1
2
3
4 dodecylsulphate (SDS, 99+% GC, Sigma-Aldrich, Japan), ruthenium tetroxide (Taab Laboratories,
5
6 Aldermaston, England), phosphotungstic acid (Agar Scientific Ltd., Stansted, UK), and
7
8 chloroform-d₁ (ISOTEC TM, Miamisburg, OH, USA).
9
10

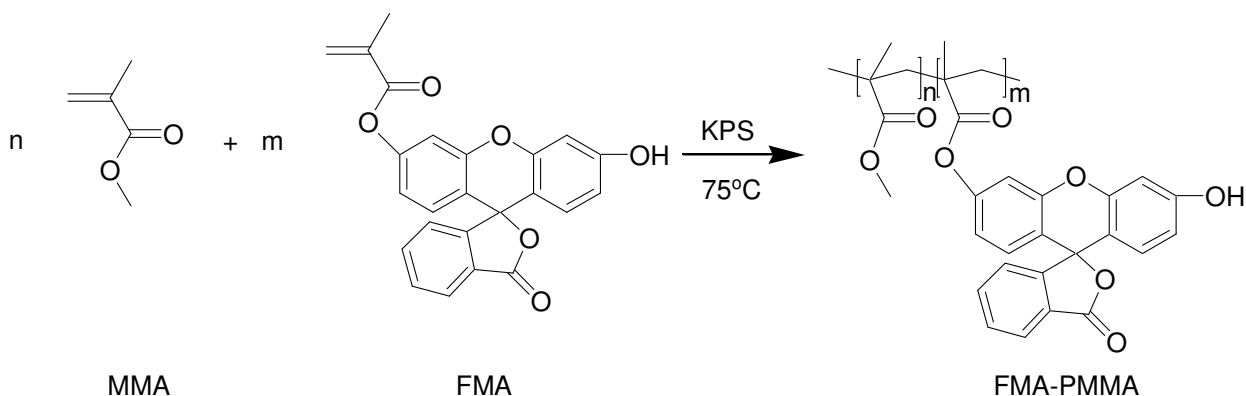
11 **Nanoparticle (NP) Preparation.** Before use, inhibitors were removed from the vinyl
12
13 monomers by passage through an alumina column. The NP were prepared in an inert nitrogen
14
15 atmosphere by free radical polymerization (see Scheme 1).
16
17
18
19
20
21
22

23 **Scheme 1.** Polymerization of styrene (Reaction A) and methyl methacrylate (MMA) (Reaction B)
24
25 with fluorescein methacrylate (FMA) using potassium persulfate (KPS) as an initiator at 75°C.
26
27

28 Reaction A:



Reaction B:



1
2
3
4
5
6
7 200 cm³ distilled water was placed in a round bottom flask, with 1 g of SDS added as an
8
9 emulsifier. The aqueous surfactant solution was deoxygenated with N₂. 13 g of deoxygenated
10
11 styrene was added into the aqueous phase. The mixture was vigorously stirred to form an emulsion
12
13 and heated to 75°C. To start the polymerization, 0.1 g KPS dissolved in a small amount of water
14
15 was added. The reaction was allowed to proceed under nitrogen for 3 hours. To prepare
16
17 fluorescently labeled NP, 0.13 g of FMA and/or 0.13 g NR were mixed with the monomer before
18
19 addition to the reaction. The same procedure was used for the preparation of PMMA NP.
20
21
22
23
24

25 **NP Characterization.** The mean size and polydispersity of the NP were measured with
26
27 dynamic light scattering (DLS BI90Plus, Brookhaven Instruments Corporation, NY, USA). The
28
29 morphology of the nanoparticles was observed on a JEOL JEM-2000 transmission electron
30
31 microscope (TEM) at an accelerating voltage of 120kV. Each sample was prepared by casting a
32
33 drop of NP dispersion onto a 300-mesh copper grid covered with carbon film. TEM images of PS
34
35 NP were obtained as positively stained preparations by placing samples in ruthenium tetroxide
36
37 vapour for 1 hour. TEM images of PMMA NP were obtained as negatively stained preparations by
38
39 placing samples in phosphotungstic acid for 1 hour. ¹H NMR spectra were recorded in deuterated
40
41 chloroform (CDCl₃) on a Bruker Avance™ III spectrometer (Billerica, MA, USA) operating at 400
42
43 MHz. Prior to analysis, the NP were washed with water and acetone to remove SDS and unreacted
44
45 compounds, and freeze-dried (Heto PowerDry PL3000, Thermo Electron corporation, Waltham,
46
47 MA, USA).
48
49
50
51
52
53
54
55

56
57 ***In vitro* Skin Permeation.** Before the experiment, the hairs were trimmed as close as possible to
58
59
60

1
2
3
4 the skin surface. Skin permeation experiments were performed in vertical Franz diffusion cells
5
6
7 thermostated at 37°C. The excised tissue was clamped between the donor and receptor compartments
8
9
10 exposing a diffusion area of 3.8 cm². The receptor compartment was filled with physiological buffer
11
12 (pH = 7.4); the donor compartment held 1 cm³ of the NP formulation and was covered with Parafilm.
13
14
15 After 6 hours of exposure, the cell was dismantled, and the skin surface was either cleaned carefully
16
17
18 with physiological buffer or was simply patted dry with tissue and then immediately visualized by
19
20
21 confocal microscopy.

22
23 **Laser Scanning Confocal Microscopy (LSCM).** The skin was examined using a LSM 510 Invert
24
25
26 Laser Scanning Microscope (Carl Zeiss, Jena, Germany). The system was equipped with an argon laser
27
28 (excitation line at 488 nm) and a HeNe laser (excitation line at 543 nm). A Plan-Neofluar 10×/0.3
29
30
31 objective, an EC Plan-Neofluar 40×/1.30 oil DIC M27 objective and a Plan-Apochromat 63×/1.40 oil
32
33
34 DIC M27 objective were used. Confocal images were obtained in the plane parallel to the sample
35
36
37 surface (xy-mode), or in the plane perpendicular (optical sectioning z-stack mode).
38
39
40
41
42
43
44
45
46
47
48
49
50
51
52
53
54
55
56
57
58
59
60

Results

NP Characterization. Table 1 summarizes the properties of the NP formulations used in the *in vitro* permeation experiments.

Table 1. Properties of the PS and PMMA nanoparticulate (NP) formulations examined^a

NP Formulation	Dyes included	Mean size (nm)	PI ^b
PS	None	28.8	0.135
PS-FMA	FMA	28.0	0.141
PS-FMA-NR	FMA and NR	30.9	0.118
PMMA	None	79.0	0.171
PMMA-FMA	FMA	99.9	0.163
PMMA-FMA-NR	FMA and NR	68.5	0.133

^a PS = polystyrene; PMMA = polymethylmethacrylate; FMA = fluorescein methacrylate; NR = Nile Red.

^b PI: polydispersity index of the size distribution (expressed using a 0-1 scale).

The NP were spherical and smooth as shown in Figure 1. The mean diameter of PS NP was less than 50 nm, while the PMMA NP were almost twice as large; these findings were confirmed by dynamic light scattering.

Proton NMR spectra of polystyrene, FMA, PMMA and the two copolymers are shown in Figure 2. Those of the copolymers show signals from either PS or PMMA and FMA even after extensive dissolution/reprecipitation, indicating that FMA is covalently bound to the polymer.

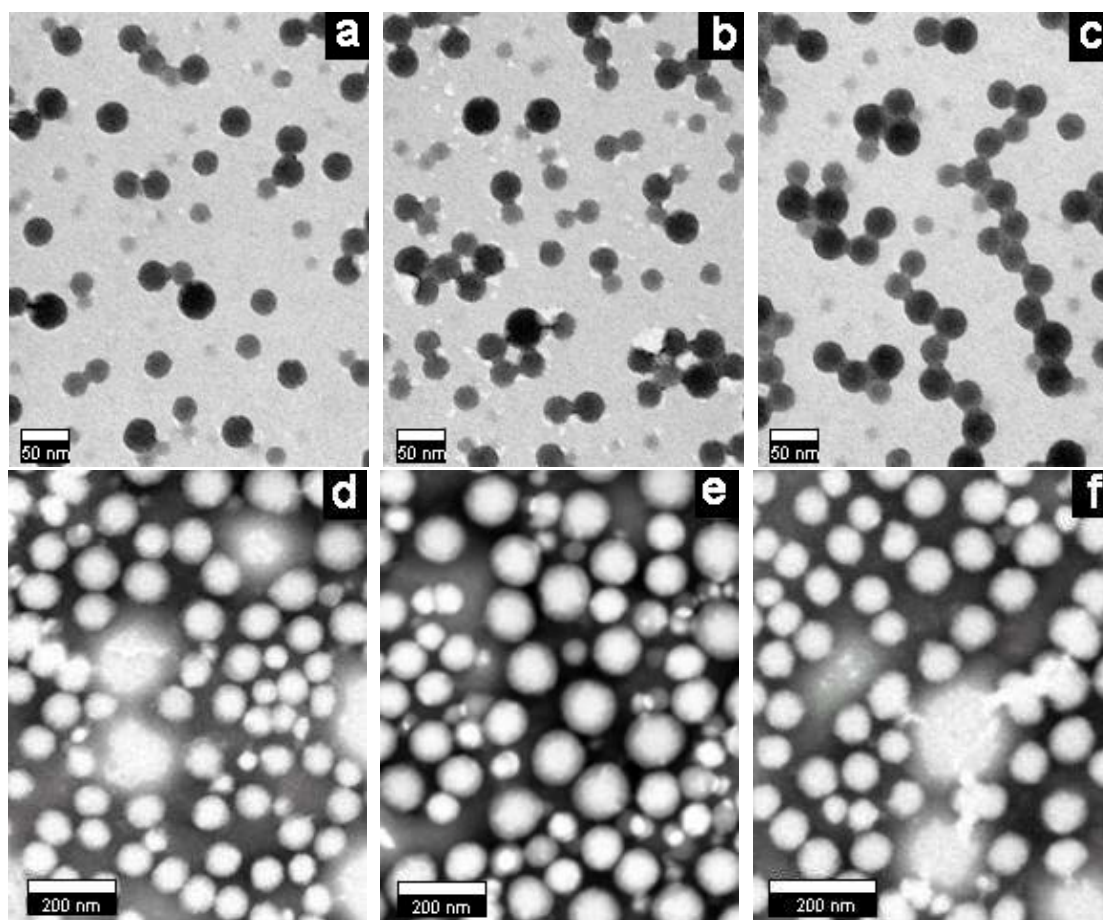
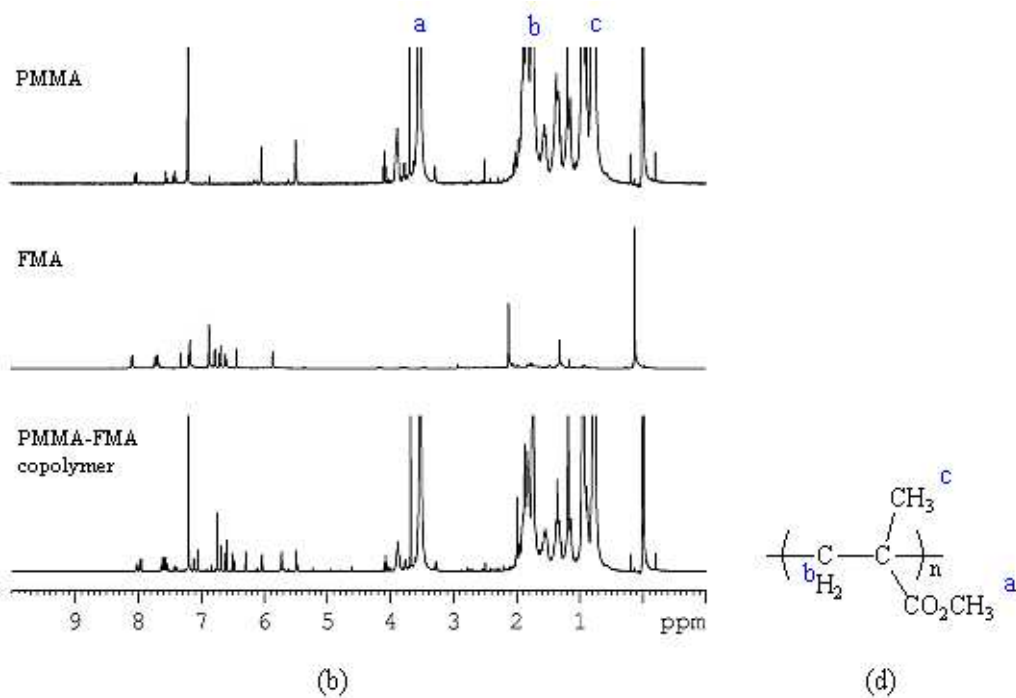
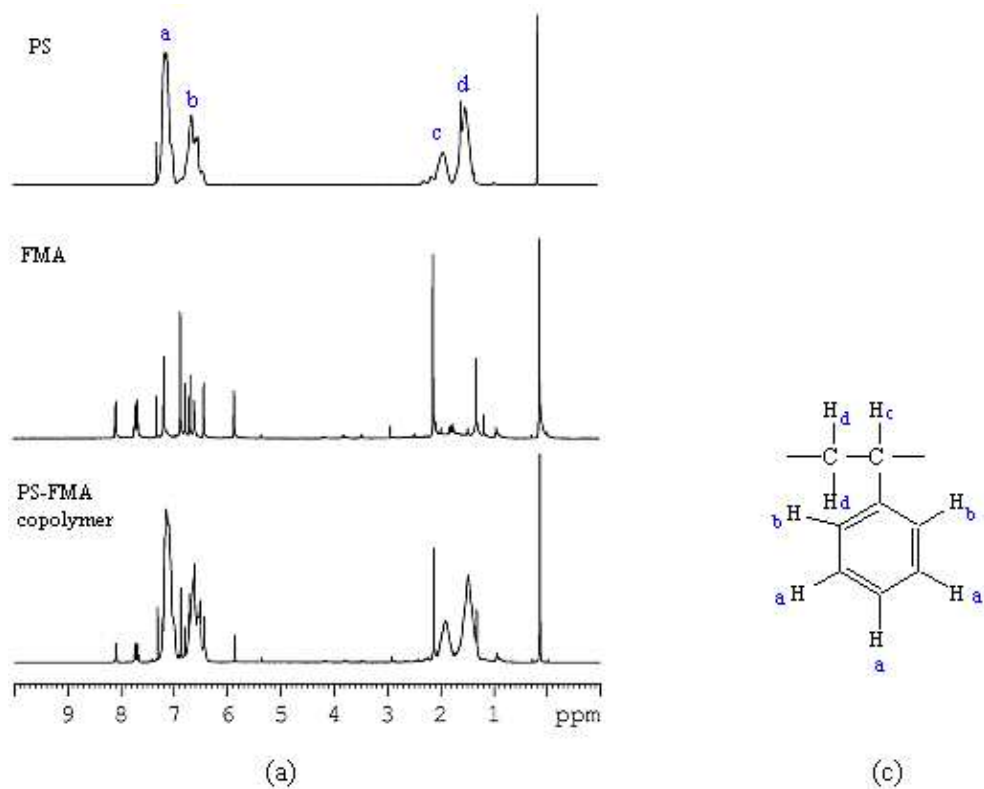


Figure 1. Transmission electron micrograph of PS and PMMA nanoparticles stained with ruthenium tetroxide (a, b and c, scale bar = 50 nm) or phosphotungstic acid (d, e, and f, scale bar = 200 nm). (a) polystyrene NP alone, (b) polystyrene with fluorescein methacrylate (FMA) polymerized, (c) polystyrene with FMA polymerized and Nile Red (NR) absorbed, (d) polymethylmethacrylate (PMMA) NP alone, (e) PMMA with FMA polymerized, and (f) PMMA with FMA polymerized and NR absorbed.



55
56
57
58
59
60

Figure 2. ^1H NMR spectra for (a) PS, FMA and PS-FMA copolymer, and (b) PMMA, FMA and PMMA-FMA copolymer, together with the structures and chemical shift assignments of (c) PS, and (d) PMMA.

1
2
3
4
5
6
7 **LSCM Images.** Nile Red is commonly used to stain intracellular lipids, because it has an
8
9 intense and stable red fluorescent emission under the excitation of HeNe laser at 543 nm. It is also a
10
11 useful model for a topical/transdermal active because of its high lipophilicity ($\log P_{o/w} > 3$)¹³ and
12
13 reasonable molecular weight (318.4 g.mol⁻¹). FMA is a fluorescent monomer containing a
14
15 polymerizable methyl acrylate functional group which can react with styrene and MMA. Under
16
17 excitation at 488 nm, FMA generates a bright green fluorescence, which locates the NP as the dye is
18
19 covalently bound to polymer. The use of NR and FMA allowed the fate of the NP and of the model
20
21 lipophilic active to be monitored independently and simultaneously in the same experiment.
22
23
24
25
26
27

28 **Control Experiments.** For each formulation, two control experiments were performed to
29
30 validate the methodology used. Firstly, PS and PMMA nanoparticle formulations without FMA
31
32 were separately applied to the skin surface. Figures 3a and 3d show the resulting confocal images,
33
34 which manifest only very weak green fluorescence that is endogenous to the SC. When the
35
36 fluorescently-labelled NP formulations were applied to the skin, distinctly different LSCM images
37
38 were observed when the skin was either cleaned properly, or not cleaned at all. Figures 3b and 3e
39
40 from the latter samples show that the NP were located in the skin furrows and around the hair
41
42 follicles. In contrast, when the skin was cleaned (Figures 3c and 3f), there was almost no residual
43
44 fluorescence, suggesting that the NP had remained at the surface and were then easily removed by
45
46 the simple washing procedure.
47
48
49
50
51
52
53
54
55
56
57
58
59
60

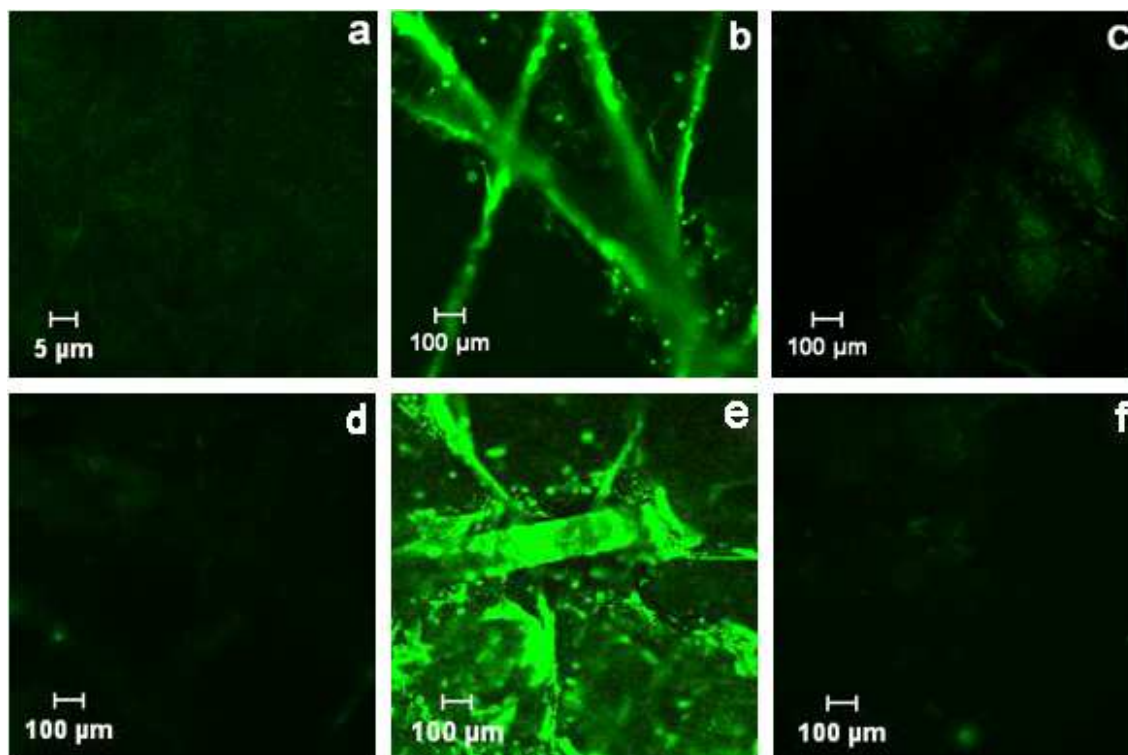
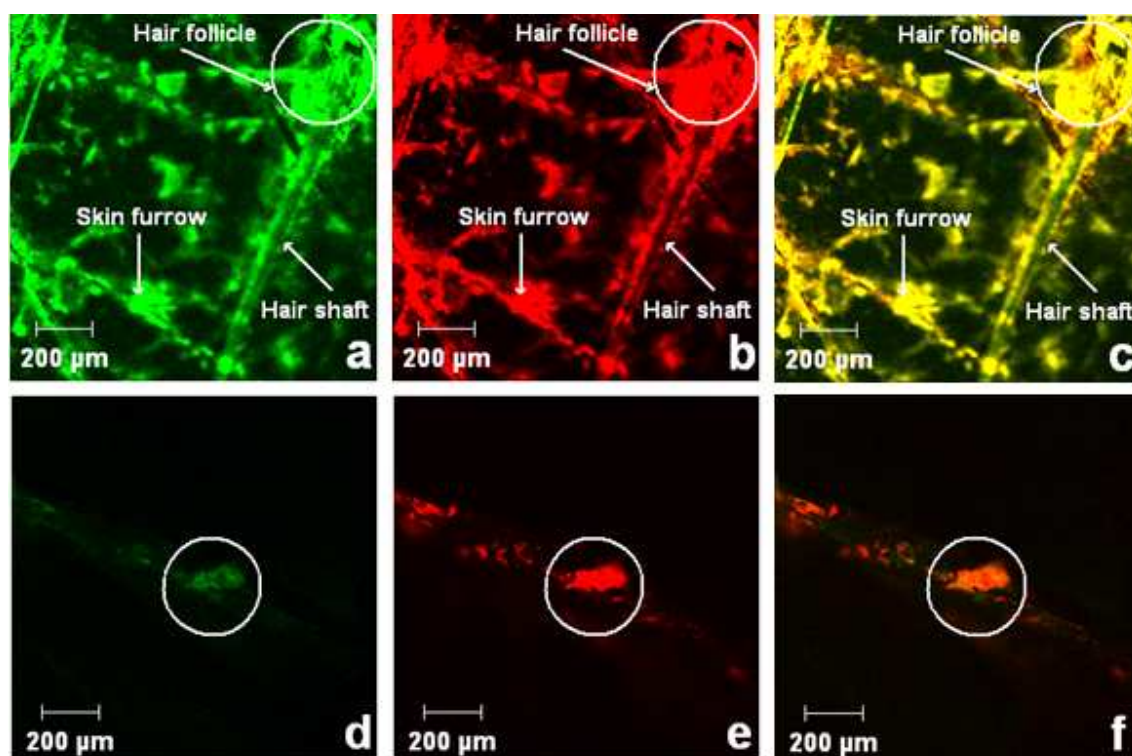


Figure 3. LSCM images of the skin surface following a 6-hour application of PS (panels a, b, c) or PMMA nanoparticles (panels d, e, f). In panels a and d, the NP were not fluorescently labelled with FMA and only a weak green fluorescence from the skin itself is seen. In panels b and e, the NP were fluorescently tagged and the skin surface was not cleaned before imaging; bright green fluorescence is apparent in the skin furrows and around the hair follicles. In panels c and f, the skin surface was cleaned before the confocal images were obtained; only the residual autofluorescence from the skin is observed, suggesting that the NP had been effectively removed by the cleaning procedure.

LSCM Images of Skin Treated with Dual-labelled Fluorescent NP without Surface

Cleaning. For skin samples treated with dual fluorophore-labelled NP formulations, LSCM images were acquired using multitracking-mode with excitation wavelengths set at 488nm and 543nm. The fluorescence emission from the two dyes was captured separately and overlaid. Figure 4 and Figure 5 illustrate the disposition of the NP and of Nile Red on and within the skin, the surface of which was not cleaned at the end of the application period, of the polystyrene and polymethylmethacrylate formulations, respectively. Location of the NP is shown by green fluorescence (from FMA

1
2
3
4 covalently attached to the polymer), while the presence of Nile Red is highlighted in red. For the
5
6
7 polystyrene formulation, NP and NR are seen on the skin surface and show clear residence in the
8
9
10 skin furrows and around the follicular openings (Figures 4a and 4b). Overlay of green and red
11
12 fluorescence in Figure 4c clearly emphasizes the co-localization of NP and active.



42
43
44
45
46
47
48
49
50
51
52
53
54

Figure 4. LSCM images ($\times 10$) from skin treated with fluorescently-labelled polystyrene NP (31 nm diameter) containing the model active NR. Panels a and b show fluorescence emission from the skin surface from the NP (panel a) and NR (panel b), respectively. Panel c shows the overlay of panels a and b and the co-localization of NP and “active” at the skin surface. Panels d and e illustrate cross-sectional images, respectively highlighting fluorescence from the NP and from NR. A distinctly labelled, short, trimmed hair is visible. Panel f is the overlay of panels d and e and suggests some permeation of released NR to the deeper skin layers.

55
56
57
58
59
60

To examine the fate of the formulation as a function of depth into the skin, the tissue was mechanically sectioned post-treatment and then examined by LSCM at a plane beyond the

mechanical section. The dispositions of NP and NR are shown in Figures 4d and 4e, respectively.

Both images highlight a short, trimmed hair shaft on which NP and NR are co-localized. Again, NP are at the surface and NR is seen there too. However, separation of NR from the nanoparticles is apparent (Figure 4f, the overlay) with some permeation of the “active” to the deeper skin layers.

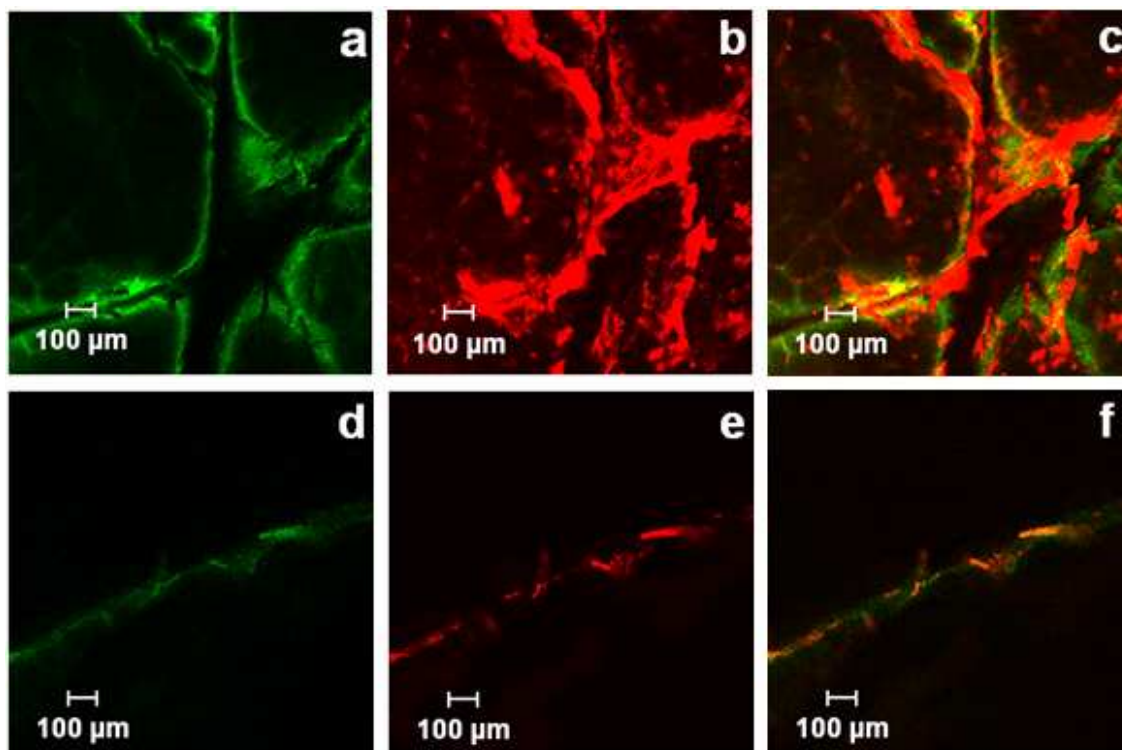


Figure 5. LSCM images ($\times 10$) from skin treated with fluorescently labelled polymethylmethacrylate NP (69 nm diameter) containing the model active NR. Panels a and b show fluorescence emission from the skin surface from the NP (panel a) and NR (panel b), respectively. Panel c shows the overlay of panels a and b, the presence of NP in the skin furrows and the release of NR from the NP at the skin surface. Panels d and e illustrate cross-sectional images, respectively highlighting fluorescence from the NP and from NR. Another short hair stub is visibly labelled. Panel f is the overlay of panels d and e and again reveals some degree of separation between NP and NR.

The corresponding images for the polymethylmethacrylate NP containing NR are in Figure 5.

Co-localization of the fluorophores in skin furrows (Figures 5a and 5b) is again observed, although

1
2
3
4 the overlay (Figure 5c) suggests that Nile Red has already been released to some extent at the skin
5
6 surface. The cross-sectioned images (Figures 5d, 5e and 5f) reveal similar behaviour and again
7
8 highlight an intensely labelled hair stub.
9
10

11 **LSCM Images of Skin Treated with Dual-labelled Fluorescent NP after Surface Cleaning.**

12
13
14 When the skin surface was properly cleaned by washing with buffer at the end of the 6-hour
15
16 experiment (as opposed to simply drying off residual solution with a paper tissue), the LSCM
17
18 images were significantly different. Using the dual-labelled polystyrene NP, post-cleaning there was
19
20 very little green fluorescence visible (Figure 6a) other than that probably attributable to skin
21
22 autofluorescence. In contrast, red fluorescence from NR was clearly visible around the corneocytes,
23
24 presumably reflecting the affinity of the lipophilic “active” for the SC intercellular lipid domains
25
26 (Figure 6b). Self-evidently, the overlay (Figure 6c) of Figures 6a and 6b reveals only the NR
27
28 released from the NP prior to their removal by the surface cleaning procedure.
29
30
31
32
33
34
35

36 Further examination of the treated skin by optically sectioning the tissue in 1 μ m steps is shown
37
38 in Figure 6d. The uptake of NR into the deeper SC is apparent. The appearance of green background
39
40 autofluorescence can also be seen and demonstrates no greater intensity than that seen in control
41
42 (untreated) samples, confirming that this signal is not due to the presence of the
43
44 fluorescently-labelled polymer (data not shown).
45
46
47
48
49
50
51
52
53
54
55
56
57
58
59
60

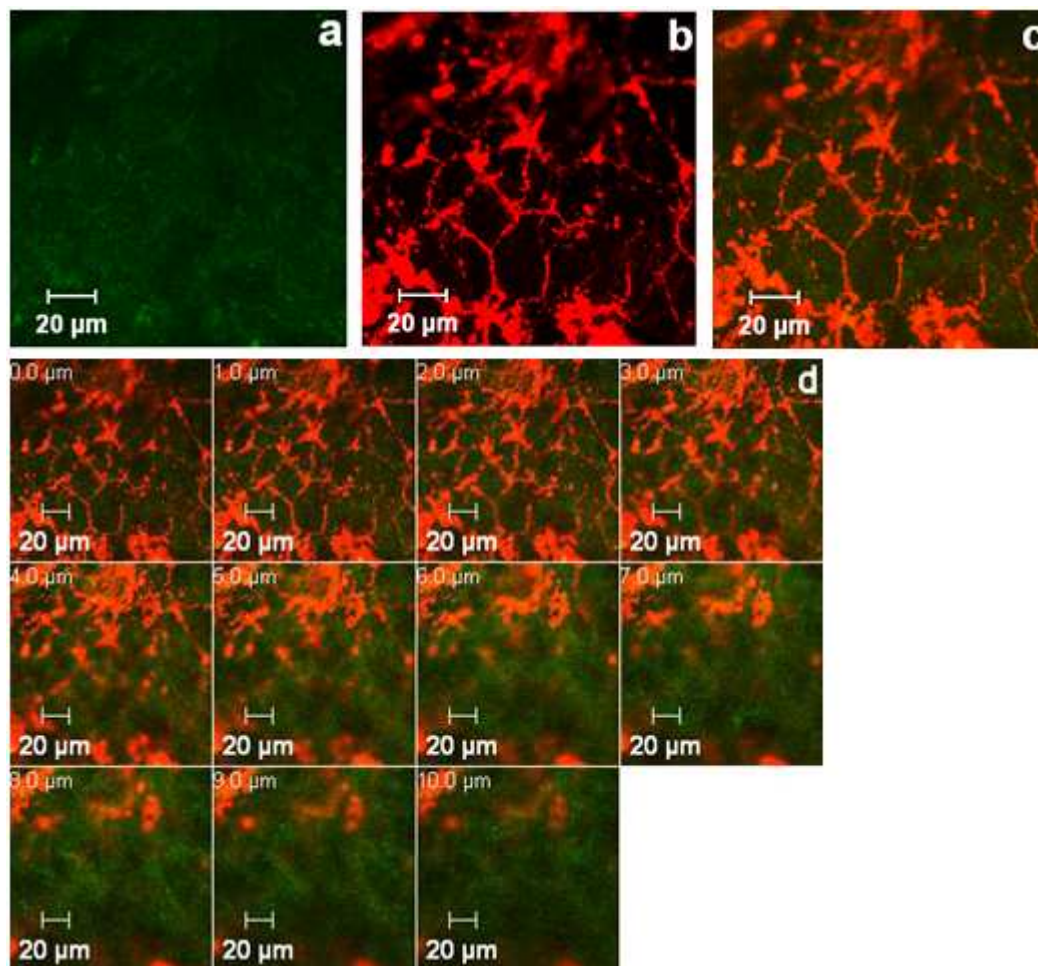
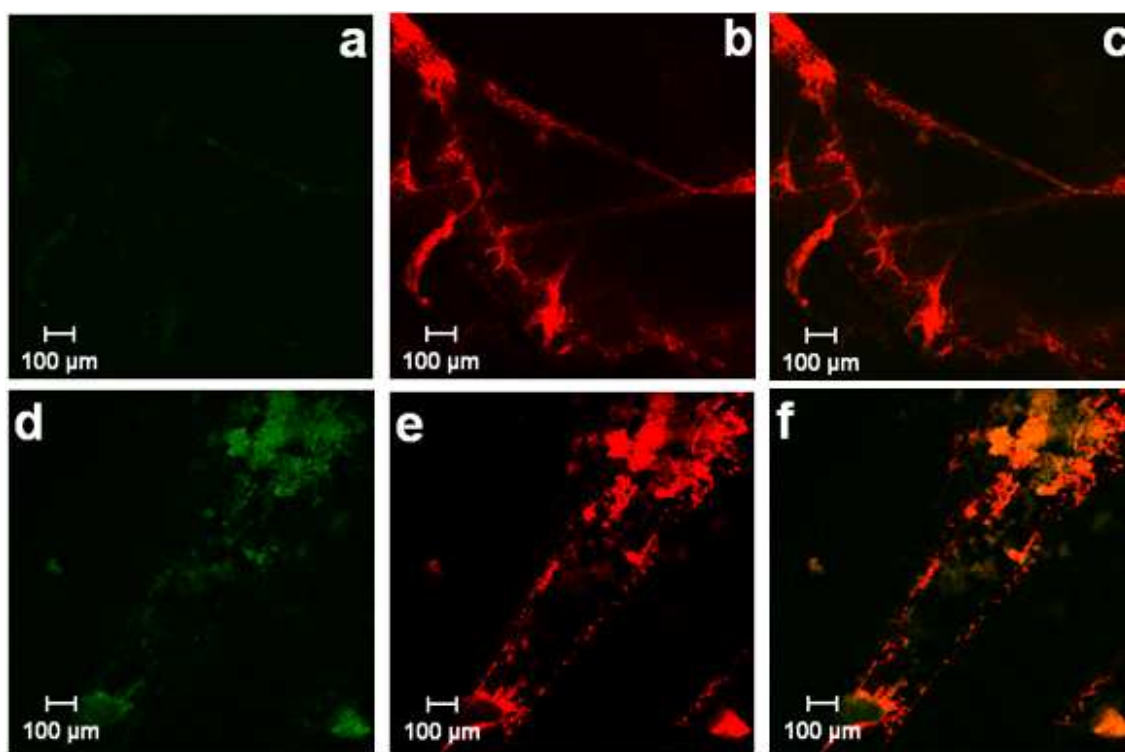


Figure 6. LSCM images ($\times 63$) from skin treated with fluorescently-labelled polystyrene NP (31 nm diameter) containing the model active. At the end of a 6-hour application, the skin surface was cleaned thoroughly with buffer and then dried. Panel a shows an almost complete absence of fluorescent NP at the surface suggesting that residual formulations had been effectively removed by washing. In contrast, panel b shows that NR had been released from the NP and had entered the lipid-rich intercellular space between the corneocytes. The overlay (panel c) and the 1 μm optical sections down to 10 μm (panel d) confirm the uptake of “active” into the deeper SC; the weak autofluorescence of the skin itself becomes progressively apparent in the later sections.

The results from the polymethylmethacrylate NP, when the skin surface is properly cleaned at the end of the application period, are similar. Figure 7a shows that no residual fluorescence from the NP is visible on the skin. On the other hand, NR has been released from the NP and has remained on/within the SC post-cleaning (Figure 7b and overlay Figure 7c). Only on hair follicles were the

1
2
3
4 NP incompletely removed by skin washing (Figure 7d), and co-localization with the “active” was
5
6
7 apparent (Figures 7e and 7f).



33
34 **Figure 7.** LSCM images from skin treated with fluorescently-labelled polymethylmethacrylate NP (69
35 nm diameter) containing NR. After a 6-hour application, the skin was thoroughly cleaned with buffer
36 and dried. Panel a shows no residual presence of NP post-washing, while panel b (and overlay panel
37 c) indicates that NR was released from the NP on/into the SC. Only on hair follicles were NP retained
38 after cleaning (panel d) and co-localization of NR on these appendages was observed (panel e and
39 overlay panel f).

40 41 42 43 44 **Discussion**

45
46 The confocal images presented in Figures 4 - 7 allow the following, principal conclusions to be
47
48 drawn: (a) NP made of polystyrene or polymethylmethacrylate do not appear able to pass beyond
49
50 the most superficial layers of the SC following a topical application lasting 6 hours; (b) the NP
51
52 show affinity for sequestration in skin furrows and on and around follicles; thorough cleaning can
53
54 remove the former but not necessarily the latter; (c) the associated hydrophobic active (NR) is
55
56
57
58
59
60

1
2
3
4 released from the NP and is able to diffuse into the deeper layers of the SC, from which it is not
5
6 removed by surface cleaning.
7

8
9 The lack of penetration of NP across intact SC is perhaps not too surprising. It is difficult to
10 envisage how a NP might traverse the SC transcellularly (which would involve uptake into
11 corneocytes and translocation through these cells). Equally, transport in the intercellular
12 channels (100 nm width) of a ~50 nm diameter particle also seems unlikely given that the
13 intercorneocyte space is filled with multiple lipid bilayers. It is also observed in our study that ~30
14 nm polystyrene nanoparticles did not penetrate beyond the SC. This observation is in agreement
15 with earlier report in the literature.¹⁴ The rigidity of the NP used in this study further undermines the
16 possibility of their permeation across the barrier, as has been suggested in earlier work comparing
17 the uptake of a lipophilic sunscreen from a nanoemulsion and from rigid NP made of cellulose
18 acetate phthalate.⁵ Parenthetically, from a practical standpoint, the fact that NP are retarded at the
19 skin surface may be a distinct advantage for a sunscreen formulation,¹⁵ especially if they are able to
20 create an occlusive film as well, from which the active may be slowly released over a prolonged
21 period.¹⁶
22
23
24
25
26
27
28
29
30
31
32
33
34
35
36
37
38
39
40
41
42
43

44 The issue of particle rigidity has also been addressed by comparing standard lipid-based
45 vesicles with specially-designed elastic species.^{17, 18} While the penetration of such elastic vesicles
46 across the entire SC has not been equivocally demonstrated, evidence for enhanced “active”
47 transport, and even for the presence of intact vesicles in deeper parts of the SC, has been reported.¹⁸
48
49
50
51
52
53
54

55 Certainly, as has been observed here, it is clear that an “active” associated with topically
56 applied NP can be released from the carrier and diffuses into the SC.^{4, 19, 20} As reported elsewhere,^{3, 6,}
57
58
59
60

1
2
3
4^{21, 22} the delivery of the “active” will depend upon its physicochemical properties, its interaction
5
6
7 with the nano-carrier, the manner of its association with the particle (surface adhesion,
8
9
10 encapsulation, or a mixture of the two), as well as the dimensions and properties (hydrophobicity,
11
12 hydrophilicity, charge, biodegradability) of the NP themselves.

13
14
15 Further work may be anticipated to explore in greater depth the potential of NP formulations to
16
17 target “actives” to the hair follicles, for example, or to create a homogeneous and substantive
18
19 surface film from which prolonged and controlled release may be achieved. Equally, while the
20
21 penetration of NP across intact SC seems unlikely to pose a toxicological concern, the risk
22
23 associated with contact to a damaged or diseased skin barrier merits considerable additional
24
25
26
27
28 research.

36 **Acknowledgements**

37
38 Supported by the European Commission 6th Research and Technological Development Framework
39
40 Programme (NAPOLEON: NAnostructured waterborne POLymEr films with OutstaNding
41
42 properties) and a University Research Scholarship for Xiao Wu.
43
44
45
46
47
48
49
50
51
52
53
54
55
56
57
58
59
60

References

1. Miyazaki, S.; Takahashi, A.; Kubo, W.; Bachynsky, J.; Loebenberg, R. Poly N-Butylcyanoacrylate (PNBCA) Nanocapsules as a Carrier for NSAIDs: In Vitro Release and in Vivo Skin Penetration. *J. Pharm. Pharmaceut. Sci.* **2003**, *6*, 238-245.
2. Luengo, J.; Weiss, B.; Schneider, M.; Ehlers, A.; Stracke, F.; Konig, K.; Kostka, K. H.; Lehr, C. M.; Schaefer, U. F. Influence of Nanoencapsulation on Human Skin Transport of Flufenamic Acid. *Skin Pharmacol. Physiol.* **2006**, *19*, 190-197.
3. Lboutounne, H.; Chaulet, J. F.; Ploton, C.; Falson, F.; Pirot, F. Sustained Ex Vivo Skin Antiseptic Activity of Chlorhexidine in Poly(ϵ -Caprolactone) Nanocapsule Encapsulated Form and as a Digluconate. *J. Controlled Release* **2002**, *82*, 319-334.
4. Alvarez-Roman, R.; Barre, G.; Guy, R. H.; Fessi, H. Biodegradable Polymer Nanocapsules Containing a Sunscreen Agent: Preparation and Photoprotection. *Eur. J. Pharm. Biopharm.* **2001**, *52*, 191-195.
5. Olvera-Martinez, B. I.; Cazares-Delgadillo, J.; Calderilla-Fajardo, S. B.; Villalobos-Garcia, R.; Ganem-Quintanar, A.; Quintanar-Guerrero, D. Preparation of Polymeric Nanocapsules Containing Octyl Methoxycinnamate by the Emulsification-Diffusion Technique: Penetration across the Stratum Corneum. *J. Pharm. Sci.* **2005**, *94*, 1552-1559.
6. Luppi, B.; Cerchiara, T.; Bigucci, F.; Basile, R.; Zecchi, V. Polymeric Nanoparticles Composed of Fatty Acids and Polyvinylalcohol for Topical Application of Sunscreens. *J. Pharm. Pharmacol.* **2004**, *56*, 407-411.
7. Oberdorster, G.; Oberdorster, E.; Oberdorster, J. Nanotoxicology: An Emerging Discipline Evolving from Studies of Ultrafine Particles. *Environ. Health Perspect.* **2005**, *113*, 823-839.
8. Oberdorster, G.; Maynard, A.; Donaldson, K.; Castranova, V.; Fitzpatrick, J.; Ausman, K.; Carter, J.;

1
2
3
4 Karn, B.; Kreyling, W.; Lai, D.; Olin, S.; Monteiro-Riviere, N.; Warheit, D.; Yang, H. Principles for
5
6 Characterizing the Potential Human Health Effects from Exposure to Nanomaterials: Elements of a Screening
7
8 Strategy. *Part. Fibre Toxicol.* **2005**, *2*, 8.

9
10
11
12 9. Borm, P. J.; Robbins, D.; Haubold, S.; Kuhlbusch, T.; Fissan, H.; Donaldson, K.; Schins, R.; Stone, V.;
13
14 Kreyling, W.; Lademann, J.; Krutmann, J.; Warheit, D.; Oberdorster, E. The Potential Risks of Nanomaterials:
15
16 A Review Carried out for Ecetoc. *Part. Fibre Toxicol.* **2006**, *3*, 11.

17
18
19
20 10. Hoet, P. H.; Bruske-Hohlfeld, I.; Salata, O. V. Nanoparticles - Known and Unknown Health Risks. *J.*
21
22 *Nanobiotechnology* **2004**, *2*, 12.

23
24
25
26 11. Sekkat, N.; Kalia, Y. N.; Guy, R. H. Biophysical Study of Porcine Ear Skin in Vitro and Its Comparison
27
28 to Human Skin in Vivo. *J. Pharm. Sci.* **2002**, *91*, 2376-2381.

29
30
31
32 12. Simon, G. A.; Maibach, H. I. The Pig as an Experimental Animal Model of Percutaneous Permeation in
33
34 Man: Qualitative and Quantitative Observations--an Overview. *Skin Pharmacol. Appl. Skin Physiol.* **2000**, *13*,
35
36 229-234.

37
38
39
40 13. Lombardi Borgia, S.; Regehly, M.; Sivaramakrishnan, R.; Mehnert, W.; Korting, H. C.; Danker, K.;
41
42 Roder, B.; Kramer, K. D.; Schafer-Korting, M. Lipid Nanoparticles for Skin Penetration
43
44 Enhancement-Correlation to Drug Localization within the Particle Matrix as Determined by Fluorescence and
45
46 Parelectric Spectroscopy. *J. Controlled Release* **2005**, *110*, 151-163.

47
48
49 14. Alvarez-Roman, R.; Naik, A.; Kalia, Y. N.; Guy, R. H.; Fessi, H. Skin Penetration and Distribution of
50
51 Polymeric Nanoparticles. *J. Controlled Release* **2004**, *99*, 53-62.

52
53
54
55 15. Nohynek, G. J.; Lademann, J.; Ribaud, C.; Roberts, M. S. Grey Goo on the Skin? Nanotechnology,
56
57 Cosmetic and Sunscreen Safety. *Crit. Rev. Toxicol.* **2007**, *37*, 251-277.
58
59
60

- 1
2
3
4 16. Magdassi, S. Delivery Systems in Cosmetics. *Colloids Surf., A: Physicochem. Eng. Aspects* **1997**,
5
6 123-124, 671-679.
7
8
9
10 17. van den Bergh, B. A.; Vroom, J.; Gerritsen, H.; Junginger, H. E.; Bouwstra, J. A. Interactions of Elastic
11
12 and Rigid Vesicles with Human Skin in Vitro: Electron Microscopy and Two-Photon Excitation Microscopy.
13
14 *Biochim. Biophys. Acta* **1999**, 1461, 155-173.
15
16
17 18. Honeywell-Nguyen, P. L.; Gooris, G. S.; Bouwstra, J. A. Quantitative Assessment of the Transport of
18
19 Elastic and Rigid Vesicle Components and a Model Drug from These Vesicle Formulations into Human Skin
20
21 in Vivo. *J. Invest. Dermatol.* **2004**, 123, 902-910.
22
23
24
25 19. Muller, B.; Kreuter, J. Enhanced Transport of Nanoparticle Associated Drugs through Natural and
26
27 Artificial Membranes--a General Phenomenon? *Int. J. Pharm.* **1999**, 178, 23-32.
28
29
30
31 20. De Campos, A. M.; Sanchez, A.; Alonso, M. J. Chitosan Nanoparticles: A New Vehicle for the
32
33 Improvement of the Delivery of Drugs to the Ocular Surface. Application to Cyclosporin A. *Int. J. Pharm.*
34
35 **2001**, 224, 159-168.
36
37
38
39 21. Rolland, A.; Wagner, N.; Chatelus, A.; Shroot, B.; Schaefer, H. Site-Specific Drug Delivery to
40
41 Pilosebaceous Structures Using Polymeric Microspheres. *Pharm. Res.* **1993**, 10, 1738-1744.
42
43
44 22. Calvo, P.; Remuñán-López, C.; Vila-Jato, J. L.; Alonso, M. J. Development of Positively Charged
45
46 Colloidal Drug Carriers: Chitosan-Coated Polyester Nanocapsules and Submicron-Emulsions. *Colloid Polym.*
47
48 *Sci.* **1997**, 275, 46-53.
49
50
51
52
53
54
55
56
57
58
59
60

Glossary of Abbreviations

DLS: dynamic light scattering

FMA: fluorescein methacrylate

KPS: potassium persulfate

LSCM: laser scanning confocal microscope

MMA: methyl methacrylate

NMR: nuclear magnetic resonance

NP: nanoparticle(s)

NR: Nile Red

PI: polydispersity index

PMMA: polymethylmethacrylate

PS: polystyrene

SC: stratum corneum

SDS: sodium dodecylsulphate

TEM: transmission electron microscope

Legends to Table, Chart, Scheme and Figures

Table 1. Properties of the PS and PMMA nanoparticulate (NP) formulations examined^a

Chart 1. Chemical structures of fluorescein methacrylate (FMA) and Nile Red (NR).

Scheme 1. Polymerization of styrene (Reaction A) and methyl methacrylate (MMA) (Reaction B) with fluorescein methacrylate (FMA) using potassium persulfate (KPS) as an initiator at 75 °C.

Figure 1. Transmission electron micrograph of PS and PMMA nanoparticles stained with ruthenium tetroxide (a, b and c, scale bar = 50 nm) or phosphotungstic acid (d, e, and f, scale bar = 200 nm). (a) polystyrene NP alone, (b) polystyrene with fluorescein methacrylate (FMA) polymerized, (c) polystyrene with FMA polymerized and Nile Red (NR) absorbed, (d) polymethylmethacrylate (PMMA) NP alone, (e) PMMA with FMA polymerized, and (f) PMMA with FMA polymerized and NR absorbed.

Figure 2. ¹H NMR spectra for (a) PS, FMA and PS-FMA copolymer, and (b) PMMA, FMA and PMMA-FMA copolymer, together with the structures and chemical shift assignments of (c) PS, and (d) PMMA.

Figure 3. LSCM images of the skin surface following a 6-hour application of PS (panels a, b, c) or PMMA nanoparticles (panels d, e, f). In panels a and d, the NP were not fluorescently labelled with

1
2
3
4 FMA and only a weak green fluorescence from the skin itself is seen. In panels b and e, the NP were
5
6
7 fluorescently tagged and the skin surface was not cleaned before imaging; bright green fluorescence
8
9
10 is apparent in the skin furrows and around the hair follicles. In panels c and f, the skin surface was
11
12
13 cleaned before the confocal images were obtained; only the residual autofluorescence from the skin
14
15
16 is observed, suggesting that the NP had been effectively removed by the cleaning procedure.
17
18
19

20 **Figure 4.** LSCM images ($\times 10$) from skin treated with fluorescently-labelled polystyrene NP (31 nm
21
22
23 diameter) containing the model active NR. Panels a and b show fluorescence emission from the skin
24
25
26 surface from the NP (panel a) and NR (panel b), respectively. Panel c shows the overlay of panels a
27
28
29 and b and the co-localization of NP and “active” at the skin surface. Panels d and e illustrate
30
31
32 cross-sectional images, respectively highlighting fluorescence from the NP and from NR. A distinctly
33
34
35 labelled, short, trimmed hair is visible. Panel f is the overlay of panels d and e and suggests some
36
37
38 permeation of released NR to the deeper skin layers.
39
40
41

42 **Figure 5.** LSCM images ($\times 10$) from skin treated with fluorescently labelled polymethylmethacrylate
43
44
45 NP (69 nm diameter) containing the model active NR. Panels a and b show fluorescence emission
46
47
48 from the skin surface from the NP (panel a) and NR (panel b), respectively. Panel c shows the
49
50
51 overlay of panels a and b, the presence of NP in the skin furrows and the release of NR from the NP
52
53
54 at the skin surface. Panels d and e illustrate cross-sectional images, respectively highlighting
55
56
57 fluorescence from the NP and from NR. Another short hair stub is visibly labelled. Panel f is the
58
59
60 overlay of panels d and e and again reveals some degree of separation between NP and NR.

1
2
3
4
5
6
7 **Figure 6.** LSCM images ($\times 63$) from skin treated with fluorescently-labelled polystyrene NP (31 nm
8 diameter) containing the model active. At the end of a 6-hour application, the skin surface was
9 cleaned thoroughly with buffer and then dried. Panel a shows an almost complete absence of
10 fluorescent NP at the surface suggesting that residual formulations had been effectively removed by
11 washing. In contrast, panel b shows that NR had been released from the NP and had entered the
12 lipid-rich intercellular space between the corneocytes. The overlay (panel c) and the 1 μm optical
13 sections down to 10 μm (panel d) confirm the uptake of “active” into the deeper SC; the weak
14 autofluorescence of the skin itself becomes progressively apparent in the later sections.
15
16
17
18
19
20
21
22
23
24
25
26
27
28
29
30

31 **Figure 7.** LSCM images from skin treated with fluorescently-labelled polymethylmethacrylate NP (69
32 nm diameter) containing NR. After a 6-hour application, the skin was thoroughly cleaned with buffer
33 and dried. Panel a shows no residual presence of NP post-washing, while panel b (and overlay panel
34 c) indicates that NR was released from the NP on/into the SC. Only on hair follicles were NP retained
35 after cleaning (panel d) and co-localization of NR on these appendages was observed (panel e and
36 overlay panel f).
37
38
39
40
41
42
43
44
45
46
47
48
49
50
51
52
53
54
55
56
57
58
59
60